



Analysis of Saint Venant Model Closure Laws from 3D Model Simulations

Amel Soualmia^{a*}, Slim Houssem Talbi^b

^aLaboratoire Science et Technologie de l'eau de l'INAT, 43 Avenue Charles Nicolle, 1082 Tunis, Tunisie

^bLaboratoire Science et Technologie de l'eau de l'INAT, 43 Avenue Charles Nicolle, 1082 Tunis, Tunisie

^aEmail: amel.inat@hotmail.fr

^bEmail: shtalbi@hotmail.fr

Abstract

In this work, in a first step, the effects of secondary motions on the transverse distribution of the depth average velocity in free surface flows above non uniform bottom roughness is illustrated by simulations based on an anisotropic algebraic Reynolds stress model (3D). These 3D-simulations were applied to determine the wall friction and the dispersion terms present in the depth average momentum equation. In a second step, closure laws of these terms were tested to define a 2D-Saint Venant model which is solved to calculate the transverse profile of the depth averaged velocity. This process could allow analyze of scale change problems.

Keywords: Secondary motions; free surface; roughness; dispersion; closure laws; the depth averaged velocity.

1. Introduction

Turbulent flow in open-channels with rough beds has been the subject of numerous experimental and computational studies due to its importance in engineering and environmental applications. For example, empirical values of boundary shear in rough channels were reported by Knight [1], and Knight, Demetriou and Hamed [2]. Recently, Chen and Chiew [3] have investigated the response of velocity and turbulence to sudden changes in bed roughness in open-channel flow.

* Corresponding author.

E-mail address: amel.inat@hotmail.fr.

In contrast to empirical studies, numerical investigations of open channels are limited because it is much more difficult to model flow in open channels than in closed conduits. Also, turbulent free surface flows present complex distribution of the bed shear stress which undulates in the transverse direction due to roughness variations of fixed or mobile beds. These bed shear patterns result from three-dimensional structures in each transverse section of the flow as a consequence of the existence of secondary currents driven by turbulence anisotropy [4]. These complexities can limit the predictive capabilities of existing free surface flow models: this is the case for 3D-models, founded on one point turbulence closures and also for 2D-Saint Venant models obtained by the depth averaging of the local equations and used currently in the field [5]. To progress in this way, in the present study, the closure problems of a 2D-Saint Venant model were analyzed using the results of 3D-simulations, with an anisotropic algebraic Reynolds stress model.

2. Mean momentum balance for fully developed flows

Fully developed flows are considered in straight rectangular open channels with constant bed slope α . Let (x, y, z) be an orthogonal coordinate system in which x and y are the longitudinal and transverse coordinates, and the z -axis is normal to the channel bottom. The components of the mean velocity and the turbulent fluctuations in the x, y and z coordinate directions are denoted by U, V, W and u, v, w , respectively. The flow being fully developed in the x -direction, all the mean quantities are only dependant on y and z coordinates and we can express the equations for the mean motion in terms of the quantities (U, Ψ, Ω) , in which Ψ and Ω are the stream function and the vorticity of secondary flows, respectively. Neglecting the effect of the viscosity the equations of U, Ψ, Ω (the 3D model) can be wrote as:

$$\frac{\partial VU}{\partial y} + \frac{\partial WU}{\partial z} = \frac{\partial}{\partial z}(-\overline{uw}) + \frac{\partial}{\partial y}(-\overline{uv}) - g \sin \alpha \quad (1)$$

$$\frac{\partial V\Omega}{\partial y} + \frac{\partial W\Omega}{\partial z} = -\frac{\partial^2}{\partial y \partial z}(\overline{w^2} - \overline{v^2}) + (\frac{\partial^2}{\partial z^2} - \frac{\partial^2}{\partial y^2})(-\overline{vw}) \quad (2)$$

$$\nabla^2 \Psi = -\Omega, \quad V = \frac{\partial \Psi}{\partial y}, \quad W = -\frac{\partial \Psi}{\partial x} \quad (3)$$

The prediction of the mean velocity field from equations (1) to (3), requires second-order closure models of the Reynolds stresses notably allowing an accurate calculation of the turbulence anisotropy term $\frac{\partial^2}{\partial y \partial z}(\overline{w^2} - \overline{v^2})$ that plays a main role in the generation of secondary flow vorticity (2). Currently used in field applications, the 2D-Saint Venant approach is founded on the introduction of depth-averaged quantities. The depth-averaging of a quantity G is denoted by $\langle G \rangle$ and defined by:

$$\mathbf{h} \langle G \rangle = \int_0^h G dz \quad (4)$$

The spatial fluctuation g'' is the difference between G and $\langle G \rangle$:

$$g'' = G - \langle G \rangle \quad \text{and} \quad \langle g'' \rangle = 0 \quad (5)$$

The depth averaging of (1) leads to the 2D-Saint Venant equation:

$$-\frac{d}{dy}(h\Phi_{SF} + h\Phi_T) + \rho hg \sin \alpha - \tau_b = 0 \quad (6)$$

Where:

$$\Phi_T = \rho \langle \overline{uv} \rangle \quad (7)$$

$$\Phi_{SF} = \rho \langle u''v'' \rangle \quad (8)$$

Where h is the water depth;

In fully developed flow, the depth-averaged quantities are only dependent on the lateral coordinate y and the differential (6) expresses the depth averaged balance of the longitudinal momentum, between the gravity force $\rho hg \sin \alpha$, the bottom friction $\tau_b = \rho u^{*2}$, and the two diffusion-dispersion terms, the depth averaged turbulent flux Φ_T and the dispersion flux Φ_{SF} due to the longitudinal momentum advection by the secondary velocity field. To predict the transverse evolution of $\langle U \rangle$, equation (6) requires closure models for the three last terms, the local shear stress velocity u^* or the local friction coefficient $C_f = (\tau_b / 0.5 \rho \langle U \rangle^2) = (2u^{*2} / \langle U \rangle^2)$ and the dispersion fluxes Φ_T and Φ_{SF} .

3. Numerical Simulations

3.1. The algebraic Reynolds stress model

In the 3D model (equations (1), (2) and (3)), the turbulent stresses were expressed by a model issued from the Reynolds stress transport model of Gibson and Rodi [6]. The components of the Reynolds tensor present in equations (1) and (2) are detailed in [4], where other precisions on this 3D model are given. In all the figures, the results of the anisotropic model are referred by the abbreviation NPF, (for Non Parallel Flow). On the same figures are also presented results obtained by assuming the flow is parallel ($V=W=0$): this case is referred by the abbreviation PF.

3.2. Boundary conditions

At the wall, $z=0$ and $0 \leq y \leq \lambda$: The longitudinal mean velocity is given by the logarithmic law. The wall boundary conditions for k and ϵ express the equilibrium between production (k) and dissipation (ϵ). At the free surface and on the lateral boundaries, symmetry conditions were imposed.

$$\frac{\partial U}{\partial y} = \frac{\partial k}{\partial y} = \frac{\partial \epsilon}{\partial y} = 0 \quad (9)$$

The boundary conditions for the secondary flow are expressed in terms of the stream function Ψ and the longitudinal vorticity Ω taken as $\Psi = 0$ and $\Omega = 0$ on the limits of the integration cross-section.

3.3. Test cases

This model was applied to Muller and Studerus [7] experiments, and to three other configurations of model roughness, in open channels of the same width, $B=0.64\text{ m}$. In these experiments, the bed forms correspond to smooth strips and rough strips of characteristic height K_S , arranged in an alternate manner as indicated in (Figure 1). Neglecting the effect of lateral walls, the simulations were limited to a symmetrical cell of length $\lambda=d_S+d_R$ situated in the central zone of the channel. In the 3D-simulations we adopted the function $C(K_S^+)$ of the roughness number $K_S^+ = ((u^*K_S) / \nu)$, which is given by the expression of Naot et Emrani [8] to account for the transition between the rough and the smooth strips:

$$C(K_S^+) = \kappa^{-1} \ln[9K_S^+ + 20](0.3K_S^{+2} + K_S^+ + 20)^{-1} \quad (10)$$

Table 1 gives the main characteristics of the open channel flows and the bed forms.

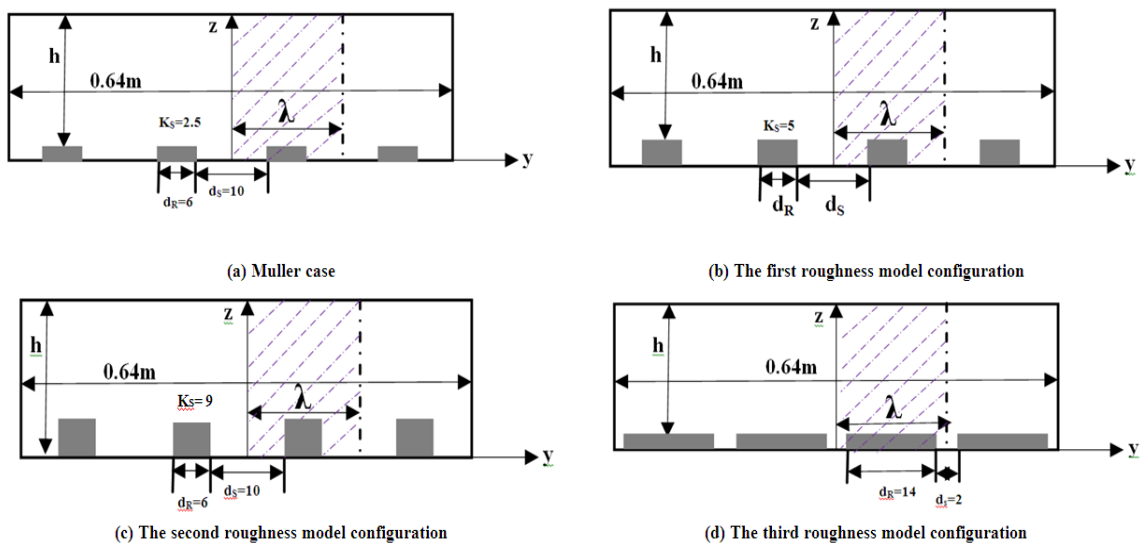


Fig. 1. shapes of the bed forms in the different roughness configurations.

Table 1. Characteristics of the open channel flows

Characteristics	Depth (cm)	Sin (α)	K_S (mm)	d_S (cm)	D_R (cm)
Muller case (a)	8	0.00143	2.5	10	6
The first roughness model configuration (b)	8	0.00143	5	10	6
The second roughness model configuration (c)	8	0.00143	9	10	6
The third roughness model configuration (d)	8	0.00143	2.5	2	14

Concerning the numerical resolution, for this 3D model, because of symmetrical conditions the simulation is considered only on the half cross section of the channel. More details could be found in [4].

4. Closure laws and resolution of the depth-averaged momentum equation (Saint Venant model)

Here we consider the closure laws of the depth-averaged equation (6), the Saint Venant model.

4.1. Closure laws

Closure assumptions have to be defined to calculate the friction coefficient C_f , the turbulent flux Φ_T and the secondary motion dispersion flux Φ_{SF} defined in (7) and (8). They were determined from the 3D-simulations with the anisotropic model, and then we attempted to define algebraic relations to express the fluxes as functions of $\langle U \rangle$. To propose a wall friction law applicable to rough, smooth and intermediate regimes, we used the logarithmic formulation developed by Labiod [9] from his experiments in a rectangular open channel with a sharp variation of the bottom roughness. He proposed the following implicit expression:

$$\sqrt{\frac{2}{C_f}} = \frac{1}{\kappa} \text{Ln}(R_e \sqrt{\frac{C_f}{2}}) + C(K_S^+) - E \tag{11}$$

In which $R_e = (\langle U \rangle h) / \nu$ and $C(K_S^+)$ is a roughness function. E is a constant, which is equal to 2.5 for our test cases. In figure 2, we plotted the transverse profiles of C_f determined in a first step from the 3D-simulations with the anisotropic model, and in a second step with the logarithmic law (11).

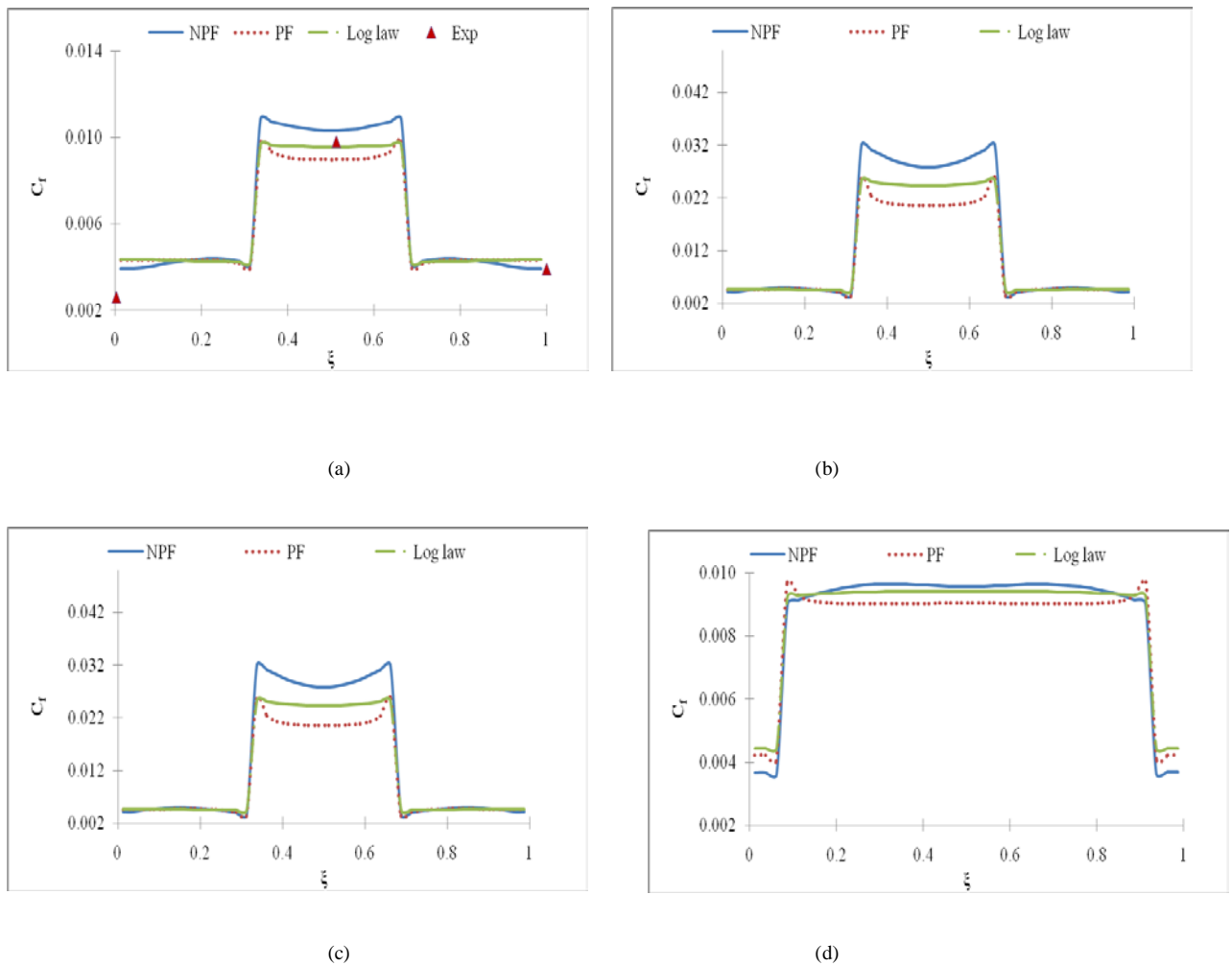


Fig. 2. Transverse distribution of the bottom friction coefficient: (a) Muller case, (b) First roughness model configuration, (c) Second roughness model configuration and (d) Third roughness model configuration.

We can observe the logarithmic law gives a good prediction of C_f above the smooth zone comparatively to NPF and PF simulation but it underestimates C_f above the rough zone ((a), (b) and (c)). On the contrary, the logarithmic law gives a good prediction of C_f above the rough zone comparatively to NPF simulation but it overestimates C_f above the smooth zone (d).

The following closures for Φ_T and Φ_{SF} were proposed:

$$\Phi_T = \rho \langle \overline{uv} \rangle = -D_T \rho u^* h \frac{d}{dy} \langle U \rangle \quad (12)$$

$$\Phi_{SF} = \rho \langle \overline{u''v''} \rangle = \lambda_{SF} \rho u^* h \frac{d}{dy} \langle U \rangle \quad (13)$$

These proposed formulations are based on the transverse gradient of the vertical mean velocity. In equations (12), and (13), D_T and λ_{SF} are constants, $D_T = 0.05$ and $\lambda_{SF} = 0.23$. These terms are calibrated by comparing these fluxes values (from (12) and (13)) and the ones issued from the 3D model. It is to note that calculations are achieved by smoothing the term $(u^* d\langle U \rangle / dy)$ to remove the discontinuities due to sharp variations of the bottom roughness.

4.2. Results of the 2D model simulations

The numerical resolution of the 2D model, equation (6), which is a second order differential equation with boundary conditions, was achieved with the closures (12), and (13), where $D_T = 0.05$ and $\lambda_{SF} = 0.23$. A finite difference method was employed. The corresponding curves are denoted by the abbreviations 2D. The 2D model presents an acceptable prediction of the transverse distribution of the mean velocity along each vertical $\langle U \rangle$ (Figure 3, where $\langle U^+ \rangle = \langle U \rangle / Um$, and Um is the section averaged velocity). In fact we note that the 2D shape curves are near the curves NPF obtained by the anisotropic 3D model. This shows the important role of the secondary flow dispersion.

We also note that the PF simulation gives a minimum and a maximum of $\langle U^+ \rangle$ above the rough and smooth zones respectively; the inverse distribution is obtained from the NPF simulation; a result which is expected, as the secondary currents are neglected. All these behaviors show the important role of the secondary flow dispersion flux Φ_{SF} , in the depth averaged equation (6).

5. Conclusions

In this paper, we analyzed the closure problems of 2D-Saint Venant equation from simulations with a 3D-model including an anisotropic algebraic Reynolds stress model. In fact the turbulent flux and the secondary motion dispersion flux were calculated by the 3D-model, to be compared to the proposed closure laws for these terms, in order to resolve the Saint Venant model, which predict the depth-averaged velocity. An acceptable agreement between the 2D and the 3D simulations was obtained. In perspective to generalize this approach of scale change, other experiments will be load and considered.

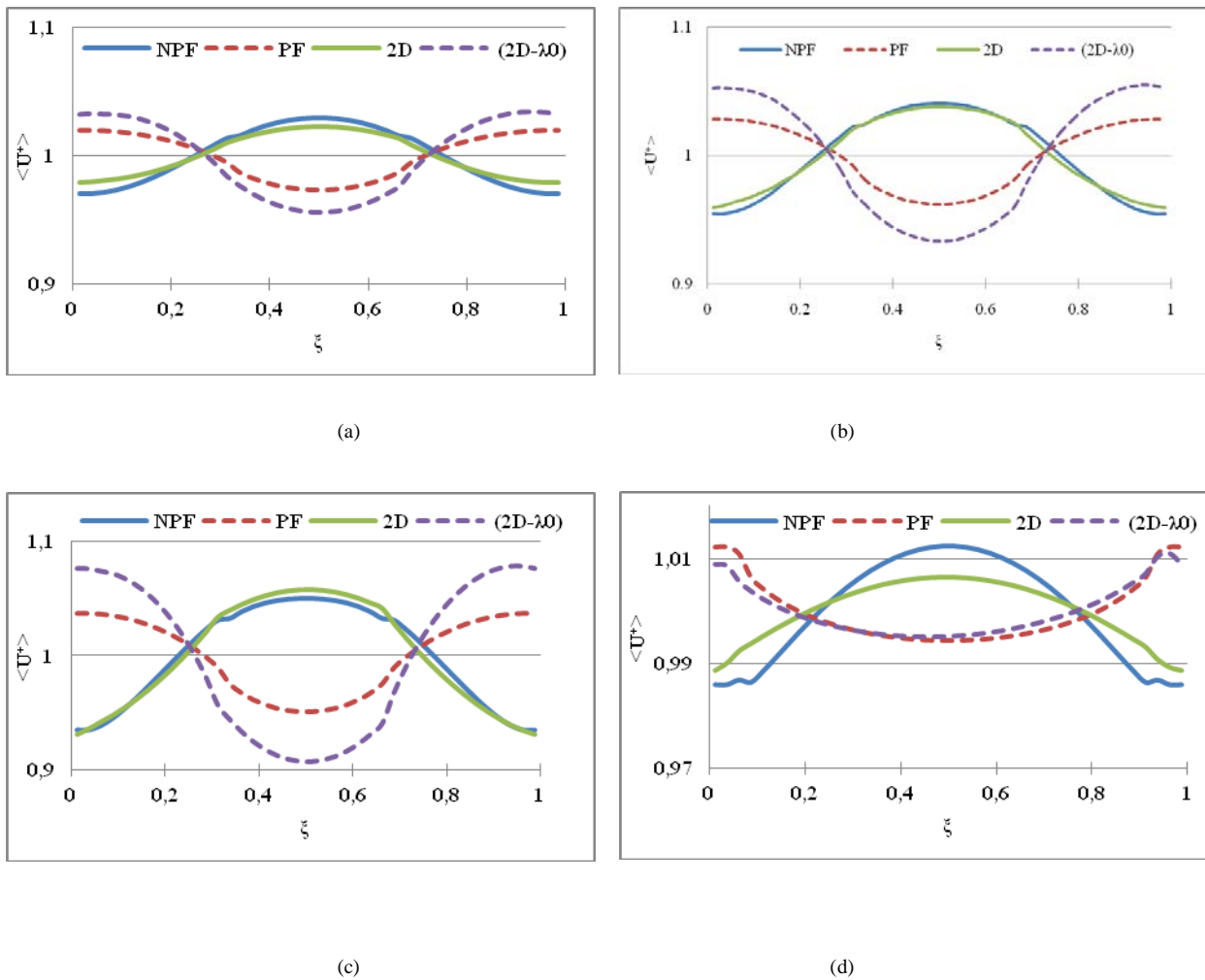


Fig. 3. Transverse distribution of non-dimensional depth averaged velocity: (a) Muller case, (b) First roughness model configuration, (c) Second roughness model configuration and (d) Third roughness model configuration.

References

- [1] D. W. Knight. "Boundary shear in smooth and rough channels." *ASCE, Journal of Hydraulic Engineering*, Hydrologic Science Division, 107 (7), pp. 839 -851, 1981.
- [2] D. W. Knight, J. D. Demetriou and M. E. Hamed. "Boundary shear in smooth rectangular channels." *ASCE, Journal of Hydraulic Engineering*, Hydrologic Science Division, 110 (4), pp. 405 -422, 1984.
- [3] X. Chen and Y. M. Chiew. "Response of velocity and turbulence to sudden change of bed roughness in open-channel flow." *Journal of Hydraulic Engineering*, 129 (1), pp. 35 -43, 2003.
- [4] A. Soualmia, L. Masbernat and A. Kaffel. "Wall friction and momentum dispersion in free surface flows with non uniform wall roughness." *Journal of PCN*, Vol, 51, pp. 11-18, 2010.

- [5] S. Bomminayuni and T, Stoesser. "Turbulence statistics in an open-channel flow over a rough bed." *Journal of Hydraulic Engineering*, 137, pp. 1347 -1358, 2011.
- [6] M. M. Gibson and W. Rodi. "Simulation of free surface effects on turbulence with a Reynolds stress model." *Journal of Hydraulic Research*, 27, pp. 233 -245, 1989.
- [7] Muller, X. Studerus. "Secondary flows in open channel." *Proceedings Congress of the International Associations for Hydraulic Research*, Italy, pp. 19-24, 1979.
- [8] D. Naot, and S. Emrani, Numerical simulation of the hydrodynamic behavior of fuel rod with longitudinal cooling fins, *Nuclear Engrs. and Des*, 73, pp. 319-329, 1983.
- [9] C. Labiod. "Etude des écoulements à surface libre sur fond rugueux. " ph.D. Thesis, INPT.IMFT, France, 2005.
- [10] S. H. Talbi and A. Soualmia. "Momentum Dispersion in Free Surface Flows through Rectangular Open-Channels with Rough Beds," presented at the 10th International Conference of Computational Methods in Sciences and Engineering (ICCMSE 2014), Athens, Greece, 2014.